Topology Preserving Thinning of Vector Fields on Triangular Meshes

Holger Theisel, Christian Rössl, and Hans-Peter Seidel

Max-Planck-Institut für Informatik, Saarbrücken, Germany
{theisel|roessl|hpseidel}@mpi-sb.mpg.de

Summary. We consider the topology of piecewise linear vector fields whose domain is a piecewise linear 2-manifold, i.e. a triangular mesh. Such vector fields can describe simulated 2-dimensional flows, or they may reflect geometric properties of the underlying mesh. We introduce a thinning technique which preserves the complete topology of the vector field, i.e. the critical points and separatrices. As the theoretical foundation, we have shown in an earlier paper that for local modifications of a vector field, it is possible to decide entirely by a local analysis whether or not the global topology is preserved. This result is applied in a number of compression algorithms which are based on a repeated local modification of the vector field – namely a repeated edge-collapse of the underlying piecewise linear domain.

1 Introduction

Topological methods have had become a standard tool for visualizing 2D vector fields because they give the opportunity to represent even complex flow structures by only a small number of graphical primitives. Since the introduction of topological methods as a visualization tool in [11], a number of extensions and modifications of topological concepts have been introduced. The original work [11] considered only first order critical points, i.e. critical points with a non-vanishing Jacobian matrix. Based on an eigenvector/eigenvalue analysis, these critical points were classified into sources, sinks and saddles. Then separatrices starting from the saddle points in the direction of the eigenvectors of the Jacobian matrix were integrated. In addition, separatrices from detachment and attachment points at no-slip boundaries were considered. [14] treats higher order critical points while [19] considers critical points at infinity. In [3], separatrices starting from boundary switch points are considered to separate regions of different inflow/outflow behavior across the boundary of the flow. [21] considers closed separatrices in the flow. Attachment and separation lines are treated in [12] as additional topological features. In [2] and [5], the topology of scalar fields is treated for visualization purposes. Initial approaches for visualizing 3D topological skeletons are presented in [9].

Flow data sets to be visually analyzed are increasingly large and increasingly complex. To deal with this problem, two general approaches have been developed which make use of topological concepts: topological simplification and topology preserving compression of vector fields.

Topology simplification methods are motivated by the assumption that not all topological features of a vector field have the same importance. This happens when some of the critical points and separatrices result from noise in the vector field. The simplest way to solve this problem is to apply a smoothing of the vector field before extracting the topology [4]. More involved techniques start with the original topological skeleton and repeatedly apply local modifications of the skeleton and/or the underlying vector field in order to remove unimportant critical points. They are based on the index theorem for vector fields which ensures that the sum of the indices of the critical points remains constant in the modified area. (See [7] or another textbook on vector analysis for an introduction to the index of critical points and the index theorem.) [3] uses an area metric to denote unimportant critical points. These points are repeatedly collapsed to more important critical points in the neighborhood. [4] collapses pairs of first order critical points of opposite index (i.e. a saddle is collapsed with a source, sink, or center). [18] uses a similar approach but provides a way of consistently updating the underlying vector field. [17] merges clusters of critical points to a higher order critical point. [20] analyzes the curvature normal of certain time surfaces to obtain a topology-preserving smoothing of a vector field. The simplification of the topology of scalar fields (which can be considered as a special case of vector field topology) is treated in [6] and [1].

Topology preserving compression techniques can be considered as a contrasting approach to topology preserving simplification techniques. Here, the complete topological skeleton is considered to be important, and compression techniques for the vector field are sought which preserve this topological skeleton completely. [13] is the first approach at an algorithm to compress a vector field under the consideration of preserving the characteristics of critical points. In [15] a method is introduced which preserves not only the critical points but also the behavior of the separatrices. Unfortunately, this approach gives reasonable compression ratios only for vector fields with a rather poor topology. An approach which gives good compression ratios even for complex topologies (under consideration of both critical points and separatrices) was recently presented in [16]. This approach is based on a theorem which shows that — although the topology of a vector field is a global feature — it can be decided entirely by a local analysis whether a local modification of the vector field is going to change the topology. Based on this, repeated local modifications of the vector field are applied which compress the data set but preserve its topology.

The vector fields we consider in this paper are piecewise linear: in the 2D domain there is a finite number of sample points in which a velocity vector is measured or simulated. To get a vector field, the sample points are trian-

gulated, and a linear interpolation is applied inside each triangle. This way, a piecewise linear vector field can be considered as a 2D triangular mesh with velocity information in each vertex. Furthermore, compression approaches for such vector fields are highly related to thinning approaches for triangular meshes. Thinning approaches reduce the number of triangles in a mesh by applying local collapsing operations. This process is steered by minimizing certain error functions between the original and the thinned mesh.

The main approach of this paper is repeatedly to apply half-edge collapses to piecewise linear vector fields (i.e. a triangular mesh) in such a way that the topology of the vector field is preserved. This approach is based on the observation that the topology reflects important properties of the vector field.

The rest of the paper is organized as follows: Sect. 2 gives a short introduction to the topology of 2D vector fields. Sect. 3 introduces a number of topology based equivalence concepts for vector fields. Based on this, Sect. 4 describes three topology preserving thinning algorithms. One of them was already presented in [16], the other two are new approaches. Sect. 5 shows the results while Sect. 6 draws some conclusions.

2 The Topology of 2D Vector Fields

The application of topological methods to a 2D vector field $\mathbf{v}$ aims to separate regions of different flow behavior in the domain of $\mathbf{v}$. To do so, the topological skeleton of $\mathbf{v}$ has to be extracted. Here we consider the following features for constructing this skeleton:

- *Critical points* [11] are isolated points with a vanishing velocity. Based on an eigenvector/eigenvalue analysis of the Jacobian of $\mathbf{v}$, we distinguish between sources, sinks, and saddles[1].
- *Boundary switch points* [3] separate outflow regions and inflow regions across the boundary of the domain of $\mathbf{v}$. (See Fig. 1a for an example.)
- *Separatrices* [11] are particular stream lines starting either from the saddle points in the direction of the eigenvectors or from the boundary switch points in both forward and backward directions.

Fig. 1b shows an example of a topological skeleton.

This system of points and lines separates the domain of $\mathbf{v}$ into regions of similar flow behavior: considering two points $\mathbf{x}_2$ and $\mathbf{x}_3$ in the same sector of the topological skeleton of $\mathbf{v}$, the stream lines passing through $\mathbf{x}_2$ and $\mathbf{x}_3$ originate in the same source or inflow region, and terminate in the same sink or outflow region. Fig. 1c and 1d give an illustration. In this paper we restrict ourselves to the topological features mentioned above. In particular

[1] There are also centre critical points, i.e. focus points of a circular flow. They are not considered in this paper because they are structurally unstable: adding some noise to a vector field, a centre becomes a source or a sink.

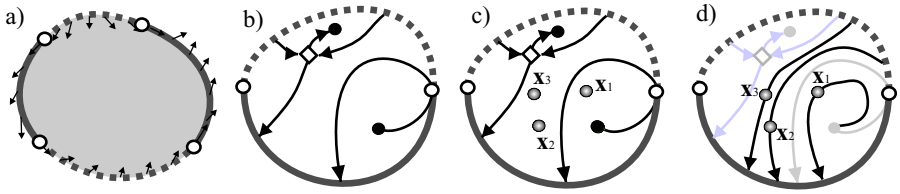

Fig. 1. a) Vector field with 2 inflow areas (dotted lines) and 2 outflow areas (solid lines) across the boundary of the domain; these areas are separated by boundary switch points (white points); b) topological skeleton of a vector field consisting of 2 boundary switch points (white points), one boundary outflow region (solid grey line), one boundary inflow region (dotted grey line), one saddle point (white diamond), one source (black point), one sink (black point), and the separatrices (black lines); c) $\mathbf{x}_2$ and $\mathbf{x}_3$ are in the same sector of the topological skeleton while $\mathbf{x}_1$ is located in a different one; d) the stream lines through $\mathbf{x}_2$ and $\mathbf{x}_3$ start in the same inflow region and end in the same outflow region while the stream line through $\mathbf{x}_1$ shows a different behaviour: it orginates at a source within the domain.

we assume that no higher order critical points [14], closed stream lines [21] or no-slip boundaries [11] appear in the flow.

3 Topologically Equivalent Vector Fields

In order to evaluate a thinning algorithm on piecewise linear vector fields, we have to compare the topological skeleton of the original and the compressed vector field. To do so, a number of topology based equivalence concepts are possible:

1. Two topological skeletons are equivalent if both their critical points and separatrices are identical.
2. Two topological skeletons are equivalent if they have the same critical points (both location and Jacobian matrices), and the corresponding separatrices end in the same critical points or inflow/outflow regions.
3. The topological skeletons of $\mathbf{v}_1$ and $\mathbf{v}_2$ are equivalent if there is a one-to-one map between the critical points of $\mathbf{v}_1$ and $\mathbf{v}_2$, such that saddles are mapped to saddles, sources to sources, and sinks to sinks, and corresponding separatrices of $\mathbf{v}_1$ and $\mathbf{v}_2$ end in corresponding critical points or inflow/outflow regions.

Note that the equivalence concept 1 is a rather strong one: $\mathbf{v}_1$ and $\mathbf{v}_2$ are supposed to have the same critical points (including the Jacobian matrices) and the same separatrices. Concept 2 relaxes this by allowing that corresponding separatrices have different paths (as long as they end in the same critical point or inflow/outflow region). In concept 3 we further relax this by allowing the critical points to move, so long as they do not merge or change their classification.

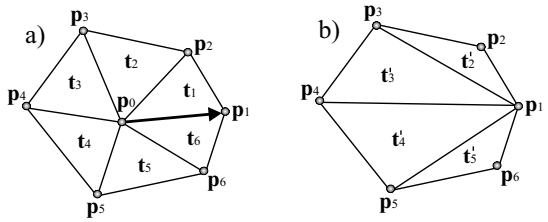

Fig. 2. Configuration for half-edge collapse $\mathbf{p}_0 \rightarrow \mathbf{p}_1$; a) triangles $\mathbf{t}_1, \ldots, \mathbf{t}_6$; b) new triangles $\mathbf{t}'_2, \ldots, \mathbf{t}'_5$.

4 Thinning the Mesh

In this section we discuss three thinning methods each preserving one of the equivalence concepts mentioned above. All these methods are based on a controlled half-edge collapse of the underlying triangular mesh. This means that a half-edge collapse is only carried out if it is guaranteed to keep the topology unchanged (using one of the equivalence concepts from Sect. 3). The whole process is a greedy optimization driven by a priority queue. In a 3D setup the priority of a collapse would be some kind of quality measure, such as distance to the original surface. In the 2D case we have an additional degree of freedom. A natural choice would be to locally apply some difference measure for flow fields [8, 10]. In our current implementation we merely assign priorities proportional to edge lengths, preferring short edges for collapse.

The core of this thinning algorithm is therefore an algorithm which decides if a particular half-edge collapse changes the topology of the whole vector field.

Consider a one-ring around a vertex $\mathbf{p}_0$ consisting of the triangles $\mathbf{t}_1, \ldots, \mathbf{t}_n$ and the vertices $\mathbf{p}_1, \ldots, \mathbf{p}_n$ (see Fig. 2a). We describe three algorithms which decide if a half-edge collapse $\mathbf{p}_0 \rightarrow \mathbf{p}_1$ (see Figs. 2a and 2b) changes the topology of $\mathbf{v}$ in the sense of one of the equivalence concepts introduced in Sect. 3.

A thinning algorithm which preserves equivalence concept 1 can easily be formulated as

Algorithm 1 *(check whether a half-edge collapse $\mathbf{p}_0 \rightarrow \mathbf{p}_1$ changes the topology in the sense of concept 1):*

1. *If one of the triangles $\mathbf{t}_1, \ldots, \mathbf{t}_n$ contains a critical point or a part of a separatrix, stop and prohibit the half-edge collapse.*
2. *Simulate the half-edge collapse $\mathbf{p}_0 \rightarrow \mathbf{p}_1$.*
3. *If one of the new triangles $\mathbf{t}'_2, \ldots, \mathbf{t}'_{n-1}$ contains a critical point, stop and prohibit the half-edge collapse.*
4. *Allow the half-edge collapse and stop.*

This algorithm is justified by the fact that any local modification is going to change the location of a critical point or a separatrix. Hence, a half-edge collapse can only be allowed in regions without any topological features.

A thinning algorithm which preserves equivalence concept 2 was introduced in [16]. There it was shown that it can be decided entirely by a local analysis of the area to be modified, whether or not a local modification (i.e. a half-edge collapse) preserves the topology. This property is remarkable because the topology of a vector field is a global feature: a local modification of a vector field might change the topology at a completely different location. In [16] it was also shown that to check whether a local modification changes the topology, a number of points on the boundary of the modified area has to be collected, and their cyclic order before and after the collapse has to be compared. This gives the following algorithm:

Algorithm 2 *(check whether a half-edge collapse* $\mathbf{p}_0 \rightarrow \mathbf{p}_1$ *changes the topology in the sense of concept 2):*

1. *Check if there are critical points inside* $\mathbf{D}' = (\mathbf{t}_1, \ldots, \mathbf{t}_n)$*. If so, prohibit the half-edge collapse and stop.*
2. *Collect all separatrices which pass through* $\mathbf{D}'$*. For each separatrix, store the entry point and exit point of* $\mathbf{D}'$ *in a cyclic list* L_1 *which is ordered in the same cyclic order as the points on the closed polygon* $((\mathbf{p}_1, \mathbf{p}_2), \ldots, (\mathbf{p}_{n-1}, \mathbf{p}_n), (\mathbf{p}_n, \mathbf{p}_1))$*.*
3. *If a separatrix enters* $\mathbf{D}'$ *more than once, prohibit the half-edge collapse*[2] *and stop.*
4. *Compute the boundary switch points of the vector field on the polygon* $((\mathbf{p}_1, \mathbf{p}_2), \ldots, (\mathbf{p}_{n-1}, \mathbf{p}_n), (\mathbf{p}_n, \mathbf{p}_1))$*, insert these points into* L_1*.*
5. *Simulate the half-edge collapse* $\mathbf{p}_0 \rightarrow \mathbf{p}_1$ *while storing the original configuration (to allow an undo of the half-edge collapse).*
6. *Apply linear interpolation of the vector field inside the new triangles* $(\mathbf{p}_1, \mathbf{p}_2, \mathbf{p}_3), (\mathbf{p}_1, \mathbf{p}_3, \mathbf{p}_4), \ldots, (\mathbf{p}_1, \mathbf{p}_{n-1}, \mathbf{p}_n))$*. Check whether there are critical points inside one of the new triangles. If so, prohibit half-edge collapse and stop.*
7. *Construct a new cyclic ordered list* L_2 *of points on the polygon* $((\mathbf{p}_1, \mathbf{p}_2), \ldots, (\mathbf{p}_{n-1}, \mathbf{p}_n), (\mathbf{p}_n, \mathbf{p}_1))$ *consisting of the following points:*
   a) *all boundary switch points from step 4 of the algorithm*
   b) *the entry points to* $\mathbf{D}'$ *of all separatrices*
   c) *the exit points, from* $\mathbf{D}'$*. These are compute by integrating the stream lines starting from all points of step 7b of this algorithm inside* $\mathbf{D}'$ *until they reach the boundary again.*
8. *Compare the cyclic order of the points in* L_1 *and* L_2*. If the corresponding points do not have the same cyclic order in* L_1 *and* L_2*, prohibit the half-edge collapse and stop.*
9. *Allow the half-edge collapse and stop.*

[2] This is necessary to fulfill the theorem in [16] on which this algorithm is based upon. In fact, the algorithm is based on the assumption that a local modification of the vector field does not change the entry points of the separatrices into the area to be modified. This does not hold any more for re-entering stream lines.

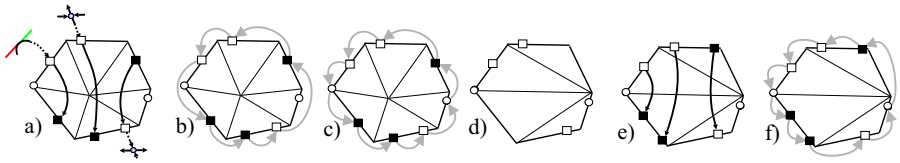

Fig. 3. Example of algorithm 2; a) 3 separatrices passing through $\mathbf{D}'$, and 2 boundary switch points (white circles) are present; the empty boxes are the entry points of the separatrices into $\mathbf{D}'$ (in integration direction), the solid boxes are the exit points; b) cyclic list L_1 (grey arrows) after step 2; c) L_1 after step 4; d) collecting points of new list L_2 after half-edge collapse: after step 7a and 7b; e) integrate new stream lines (step 7c); f) cyclic list L_2 after step 7c; half-edge collapse is allowed, since the corresponding points in L_1 and L_2 (shown in c) and f)) are in the same order.

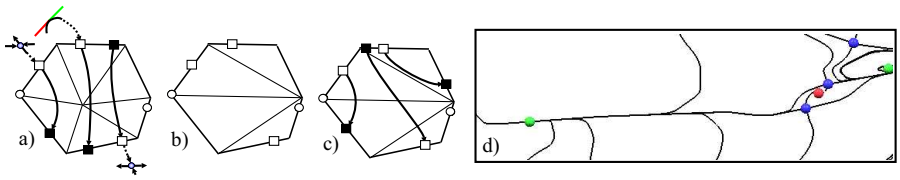

Fig. 4. a) Another example of algorithm 2; a) 3 separatrices passing through $\mathbf{D}'$, and 2 boundary switch points (white circles) are present: L_1 consists of the marked points on the boundary; b) points of L_2 after step 7b; c) points of L_2 after step 7c; edge collapse is not allowed, since the corresponding points in L_1 and L_2 (shown in a) and c)) are in a different order; d) example of separatrices which tend to be very close to each other.

Fig. 3 illustrates an example of this algorithm where an edge collapse is allowed. Figs. 4a – 4c show an example where the algorithm prohibits a half-edge collapse.

Now we want to modify algorithm 22 to handle equivalence concept 3. To do so, we have to compare the critical points in $\mathbf{D}'$ before and after the half-edge collapse if some of the critical points collapsed. We get the following

Algorithm 3 *(check whether a half-edge collapse* $\mathbf{p}_0 \rightarrow \mathbf{p}_1$ *changes the topology in the sense of concept 3):*

1. *Extract and store the critical points inside* $\mathbf{D}' = (\mathbf{t}_1, \ldots, \mathbf{t}_n)$. *If there is more than one saddle, or if there is more than one source/sink, then prohibit the half-edge collapse and stop.*
2. *as in algorithm 2.*
3. *as in algorithm 2.*
4. *as in algorithm 2.*
5. *as in algorithm 2.*
6. *Apply linear interpolation of the vector field inside the new triangles* $(\mathbf{p}_1, \mathbf{p}_2, \mathbf{p}_3), (\mathbf{p}_1, \mathbf{p}_3, \mathbf{p}_4), \ldots, (\mathbf{p}_1, \mathbf{p}_{n-1}, \mathbf{p}_n)$). *Check the new triangles for*

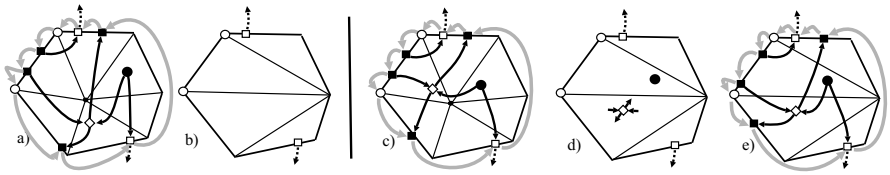

Fig. 5. a) 1-ring containing one saddle (white diamond) and one source (black circle); 3 of the 4 separatrices created by the saddle leave the 1-ring while one ends in the source; in addition, two separatrices enter the region from outside (hollow boxes): one ends in the source, the other leaves the region; b) simulated half-edge collapse removes the critical points: half-edge collapse is not allowed; c) another example of a 1-ring containing one saddle (white diamond) and one source (black circle); d) simulated half-edge collapse gives two new critical points: one saddle and one sink; e) cyclic list L_2 after step 7 of algorithm 3; e) the half-edge collapse is allowed.

critical points. If the number of saddles or the number of sources/sinks does not coincide with the numbers found in step 1, prohibit the half-edge collapse and stop. If there is one saddle, integrate its 4 separatrices until they leave $\mathbf{D}'$*. Store the 4 exit points into a new cyclic list* L_2 *of points on the polygon* $((\mathbf{p}_1, \mathbf{p}_2), \ldots, (\mathbf{p}_{n-1}, \mathbf{p}_n), (\mathbf{p}_n, \mathbf{p}_1))$.

7. *Insert the following points into* L_2*:*
   a) *as in algorithm 2.*
   b) *as in algorithm 2.*
   c) *as in algorithm 2.*
8. *as in algorithm 2.*
9. *as in algorithm 2.*

Figs. 5a and 5b illustrate an example of algorithm 3 where the half-edge collapse is not allowed. Figs. 5c – 5e show an example with an allowed half-edge collapse.

An analysis of the algorithm in [16], especially on the skin friction data set (described in the next section), had shown that this data set tends to have many separatrices very close to each other (see Fig. 4d for an example). This can be explained with the presence of attachment and separation lines [12]. For these cases the algorithm in [16] may forbid a half-edge collapse due to numerical instabilities. To solve this, we collected the entry points of separatrices at the 1-ring of a vertex to clusters: entry points of separatrices which are very close to each other[3] are set to the same entry point and thus have the same exit point as well.

[3] We used 1/1000 of the length of the boundary edge.

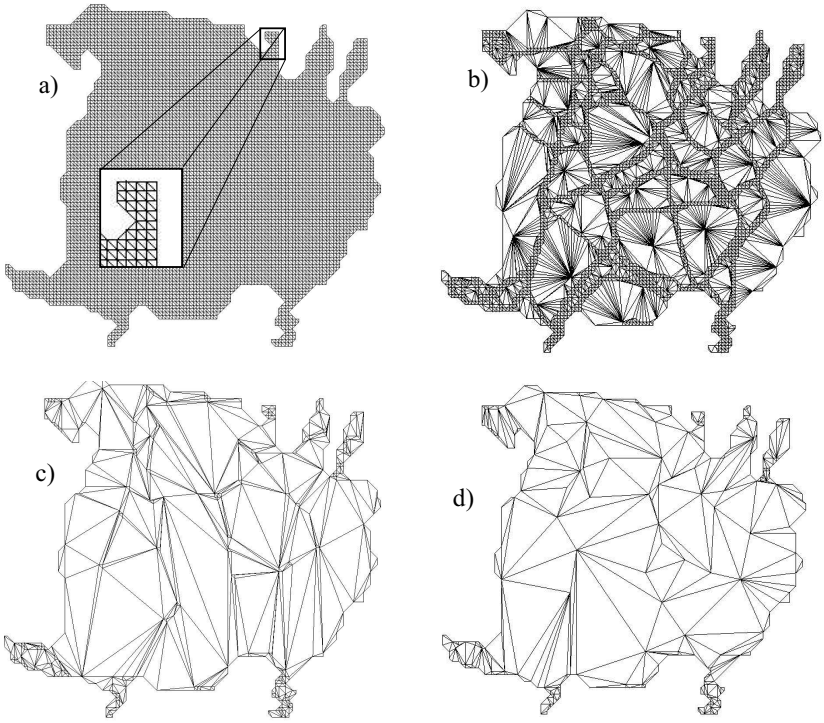

Fig. 6. Test data set 1 (flow in a bay area near Greifswald); a) piecewise triangular domain of the original data set; b) domain of the compressed data set (algorithm 1); c) domain of the compressed data set (algorithm 2); d) domain of the compressed data set (algorithm 3).

5 Results

We applied our thinning algorithms to two test data sets. The first data set describes (the perpendicular of) the flow of a bay area of the Baltic Sea near Greifswald in Germany. The data set was created by the Department of Mathematics, University of Rostock. The data is given as an incomplete flow data set on a regular 115 x 103 grid. Triangulating the defined cells, we have a piecewise linear vector field consisting of 14,086 triangles (see Fig. 6a). Fig. 7a shows the topological skeleton of the vector field. This flow data set consists of 71 critical points, 44 boundary switch points, and 168 separatrices. Fig. 6b shows the resulting triangular grid after applying algorithm 1. This grid consists of 4,944 triangles. We can clearly see that areas containing separatrices or critical points are left untouched by the algorithm. Fig. 7b shows the topological skeleton after algorithm 1 (which by definition has to be identical to Fig. 7a).

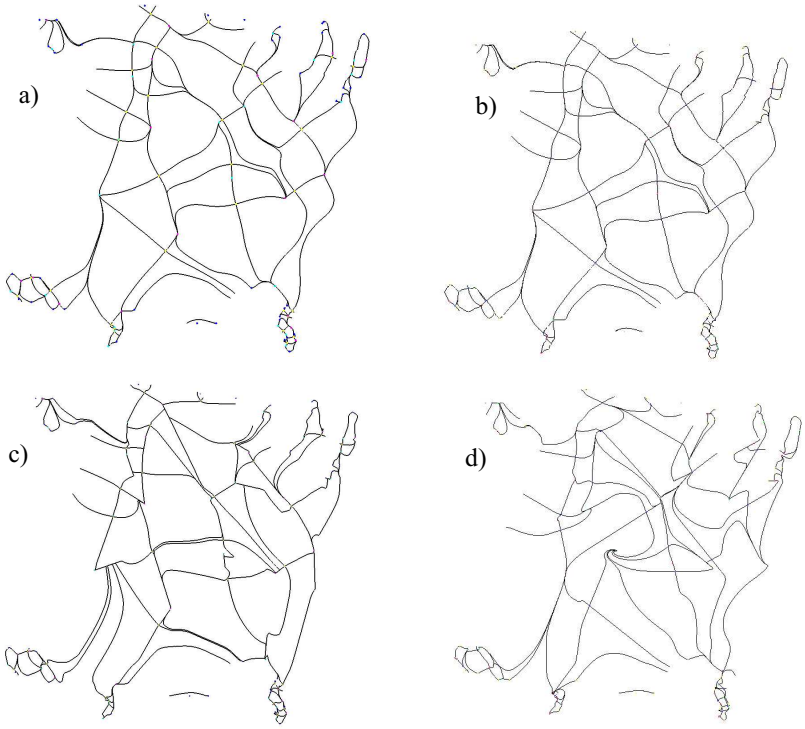

Fig. 7. Test data set 1; a) topological skeleton of original data set; b) topological skeleton of compressed data set (algorithm 1); c) topological skeleton of compressed data set (algorithm 2); d) topological skeleton of compressed data set (algorithm 3).

Applying algorithm 2, we obtained a new piecewise linear vector field which consists of 660 triangles. Fig. 6c shows the piecewise triangular domain of the compressed vector field. Fig. 7c shows the topological skeleton of the compressed vector field. The compression ratio is 95.3%. The complete compression algorithm took 280 seconds on an Intel Xeon 1.7 GHz processor. Figs. 6d and 7d show the same results for algorithm 3. Here, the number of triangles was reduced to 374. Fig. 6d shows the resulting triangular grid while Fig. 7d shows the new topological skeleton.

The second test data set describes the skin friction on a face of a cylinder which was obtained by a numerical simulation of a flow around a square cylinder. The data set was generated by Verstappen and Veldman of the University of Groningen. This data set is also analyzed in [3],[13] and [16]. The data is given on a rectangular 102 x 64 grid with varying grid size. To get a piecewise linear vector field, we divided each grid cell into two triangles which gives a piecewise triangular domain consisting of 12,726 triangles. Fig. 8a shows the piecewise triangular domain of the vector field. As we can see in this picture,

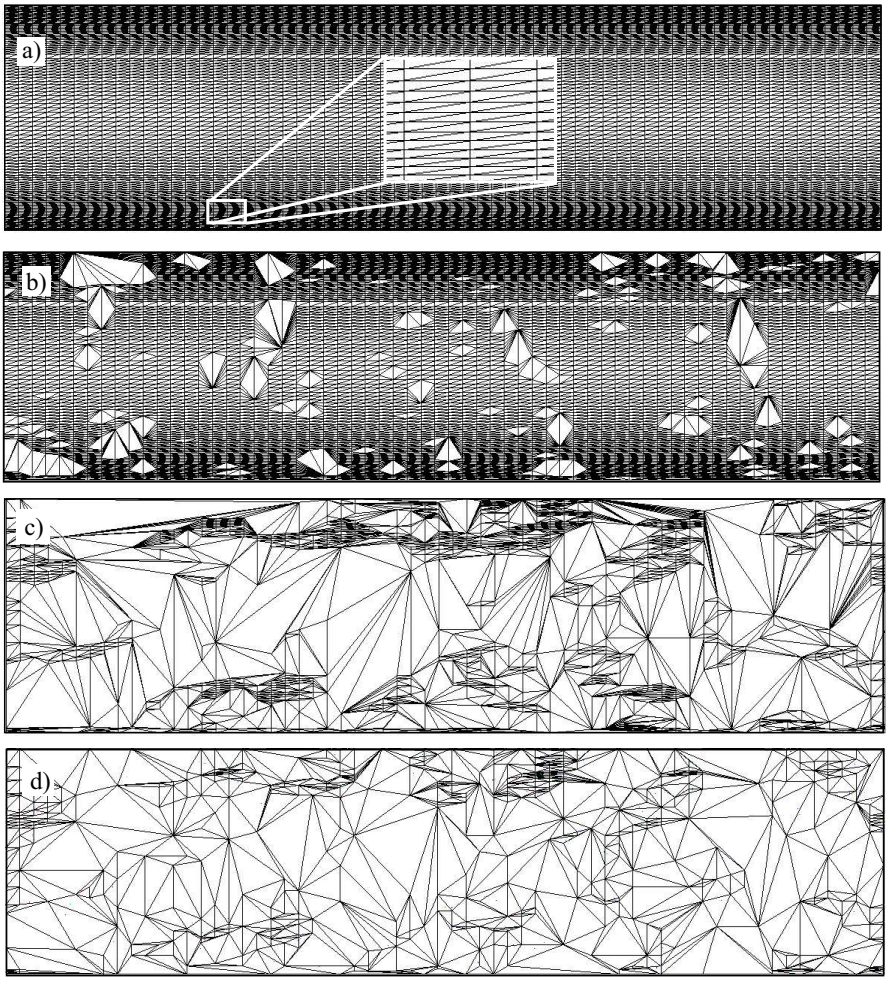

Fig. 8. Test data set 2 (skin friction); a) piecewise triangular domain of the original data set; b) domain of the compressed data set (algorithm 1); c) domain of the compressed data set (algorithm 2); d) domain of the compressed data set (algorithm 3).

all triangles there tend to be long and thin. Fig. 9a shows the topological skeleton of the vector field. This vector field consists of 338 critical points, 34 boundary switch points, and 714 separatrices. Therefore, it can be considered as a vector field of complex topology. Fig. 8b shows the resulting grid after applying algorithm 1. This grid consists of 10,680 triangles. As we can see, almost no thinning took place because the separatrices of this vector field are rather dense. Fig. 9b shows the topological skeleton after algorithm 1 (identical to Fig. 9a). By applying our compression algorithm 2, we obtained a vector field

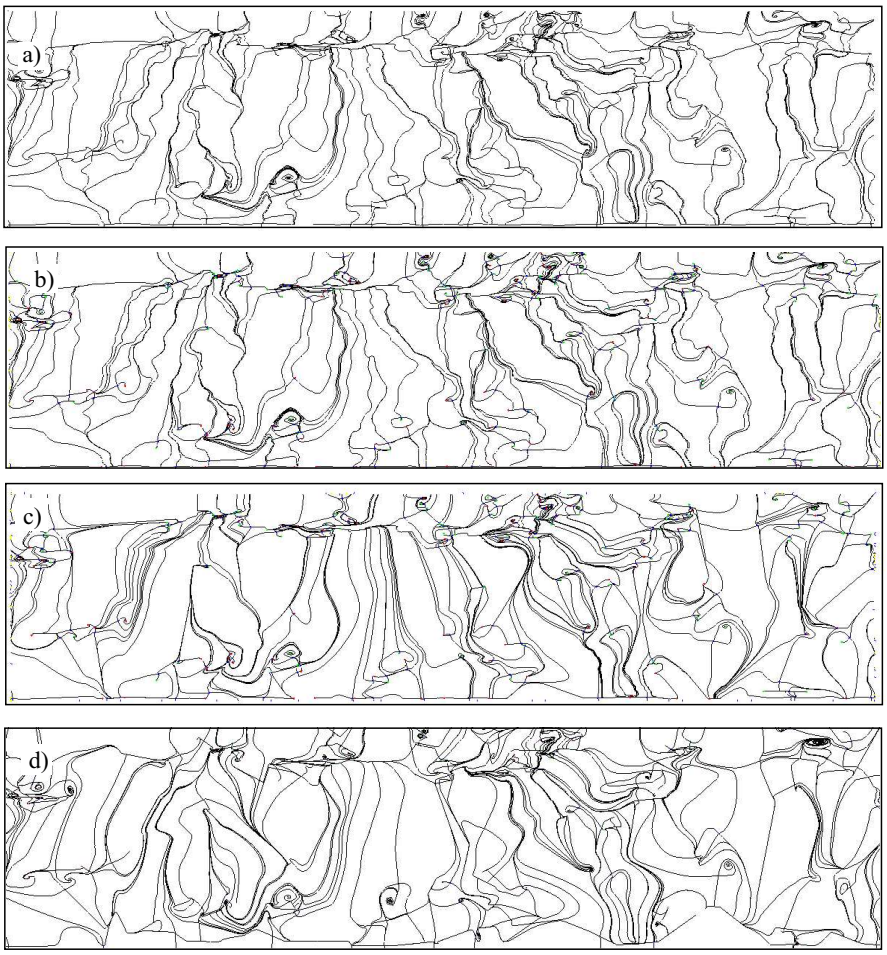

Fig. 9. Test data set 2 (skin friction); a) topological skeleton of original data set; b) topological skeleton of compressed data set (algorithm 1); c) topological skeleton of compressed data set (algorithm 2); d) topological skeleton of compressed data set (algorithm 3).

with the piecewise triangular domain shown in Fig. 8c. This domain consists of 2,153 triangles which gives a compression ratio of 83.1%. Fig. 9c shows the topological skeleton. The complete compression algorithm took 299 seconds on an Intel Xeon 1.7 GHz processor. Fig. 8d shows the underlying grid resulting from algorithm 3 consisting of 1071 triangles. The topological skeleton of this vector field is shown in Fig. 9d.

6 Conclusions

We have introduced and compared a number of new topology preserving thinning algorithms for piecewise linear vector fields which are based on one of the topology based equivalence concepts of Sect. 3. We applied the algorithms to two test data sets of moderate and complex topology respectively.

Equivalence concept 1 (and its thinning algorithm) gives very poor compression ratios for topologically complex data. This is due to the fact that the appearance of a critical point or separatrix in a triangle prevents it from being collapsed.

Equivalence concept 2 gives significant compression ratios even for topologically complex data sets. Applying this algorithm guarantees that the topological skeleton of the original and the thinned vector field coincide in the critical points and the connectivity of the separatrices.

In comparison to equivalence concept 2, concept 3 gives a further reduction of the number of triangles in the thinned mesh by a factor of approximately 50%. This was achieved for both test data sets. The visualization of the topological skeleton shows that the critical points change their locations, but the change tends to be limited to the neighborhood of the original critical point.

Acknowledgements

The authors thank Wim de Leeuw for providing the second test data set. This work was supported in part by the European Union research project "Multiresolution in Geometric Modelling (MINGLE)" under grant HPRN–CT–1999–00117.

References

1. C. Bajaj and D. Schikore. Topology-preserving data simplification with error bounds. *Comput. & Graphics*, 22(1):3–12, 1998.
2. C. L. Bajaj, V. Pascucci, and D. R. Schikore. Visualization of scalar topology for structural enhancement. In *Proc. IEEE Visualization '98*, pages 51–58, 1998.
3. W. de Leeuw and R. van Liere. Collapsing flow topology using area metrics. In *Proc. IEEE Visualization '99*, 1999.
4. W. de Leeuw and R. van Liere. Visualization of global flow structures using multiple levels of topology. In *Data Visualization 1999. Proc. VisSym 99*, pages 45–52, 1999.
5. T. K. Dey, H. Edelsbrunner, S. Guha, and D. V. Nekhayev. Topology preserving edge contraction. *Publ. Inst. Math (Beograd)*, 66(1999):23–45, 1999.
6. H. Edelsbrunner, J. Harer, and A. Zomorodian. Hierarchical Morse complexes for piecewise linear 2-manifolds. In *Proc. 17th Sympos. Comput. Geom. 2001*, 2001.
7. P. A. Firby and C. F. Gardiner. *Surface Topology*, chapter 7, pages 115–135. Ellis Horwood Ltd., 1982. Vector Fields on Surfaces.

8. H. Garcke, T. Preusser, M. Rumpf, A. Telea, U. Weikardt, and J. van Wijk. A continuous clustering method for vector fields. In T. Ertl, B. Hamann, and A. Varshney, editors, *Proc. IEEE Visualization 2000*, pages 351–358, 2000.
9. A. Globus and C. Levit. A tool for visualizing of three-dimensional vector fields. In *Proc. IEEE Visualization '91*, pages 33–40. IEEE Computer Society Press, 1991.
10. B. Heckel, G.H. Weber, B. Hamann, and K.I.Joy. Construction of vector field hierarchies. In D. Ebert, M. Gross, and B. Hamann, editors, *Proc. IEEE Visualization '99*, pages 19–26, Los Alamitos, 1999.
11. J. Helman and L. Hesselink. Representation and display of vector field topology in fluid flow data sets. *IEEE Computer*, 22(8):27–36, August 1989.
12. D. N. Kenwright, C. Henze, and C. Levit. Feature extraction of separation and attachment lines. *IEEE Transactions on Visualization and Computer Graphics*, 5(2):135–144, 1999.
13. S. K. Lodha, J. C. Renteria, and K. M. Roskin. Topology preserving compression of 2D vector fields. In *Proc. IEEE Visualization 2000*, pages 343–350, 2000.
14. G. Scheuermann, H. Krüger, M. Menzel, and A. Rockwood. Visualizing nonlinear vector field topology. *IEEE Transactions on Visualization and Computer Grapics*, 4(2):109–116, 1998.
15. H. Theisel. Designing 2D vector fields of arbitrary topology. *Computer Graphics Forum (Eurographics 2002)*, 21(3):595–604, 2002.
16. H. Theisel, C. Rössl, and H.-P. Seidel. Compression of 2D vector fields under guaranteed topology preservation. *Computer Graphics Forum (Eurographics 2003)*, 22(3):333–342, 2003.
17. X. Tricoche, G. Scheuermann, and H. Hagen. A topology simplification method for 2D vector fields. In *Proc. IEEE Visualization 2000*, pages 359–366, 2000.
18. X. Tricoche, G. Scheuermann, and H. Hagen. Continuous topology simplification of planar vector fields. In *Proc. Visualization 01*, pages 159 – 166, 2001.
19. I. Trotts, D. Kenwright, and R. Haimes. Critical points at infinity: a missing link in vector field topology. In *Proc. NSF/DoE Lake Tahoe Workshop on Hierarchical Approximation and Geometrical Methods for Scientific Visualization*, 2000.
20. R. Westermann, C. Johnson, and T. Ertl. Topology-preserving smoothing of vector fields. *IEEE Transactions on Visualization and Computer Graphics*, 7(3):222–229, 2001.
21. T. Wischgoll and G. Scheuermann. Detection and visualization of closed streamlines in planar flows. *IEEE Transactions on Visualization and Computer Graphics*, 7(2):165–172, 2001.